Green Chemistry

PAPER

View Article Online
View Journal | View Issue

Check for updates

Cite this: *Green Chem.*, 2022, **24**, 2624

Environmentally sustainable, high-performance lignin-derived universal adhesive†

Sandip K. Singh, Kolja Ostendorf, Markus Euring and Kai Zhang*

Received 3rd January 2022,
Accepted 25th February 2022

DOI: 10.1039/d2gc00014h

rsc.li/greenchem

The production of unfavorable formaldehyde-based adhesives could be replaced by that of lignin-based adhesives as an improved, healthy and sustainable candidate. Here, a facile method was realized for a novel lignin-based, robust, and universally applicable adhesive (84% yield), based on the synergistic reaction between lignin, dimethylformamide, and acrylic acid under a basic environment. Characterization studies of the synergistically synthesized lignin-based adhesive showed the formation of new C–O, C–N, and C–C bonds. These bonds contributed strongly to excellent adhesive performance on versatile substrates, including glass, aluminum, stainless steel, polycarbonate, polyvinyl chloride, and wood. This universal adhesive was able to hold vertically or horizontally >2.0 × 10^5 times its own weight for more than 94 d. It also exhibited excellent storage and loss modulus, internal bond strength (255.0 kPa), and physical-mechanical strength under neutral, acidic (pH 3.08) or basic (pH 10.22) media. These advantages enable this lignin-based adhesive to be a universal adhesive in various settings.

Open Access Article. Published on 25 February 2022. Downloaded on 1/23/2026 6:06:52 PM.
This article is licensed under a Creative Commons Attribution-NonCommercial 3.0 Unported Licence.

Introduction

After a century of robust and flourishing growth of phenolic resins, phenol and formaldehyde are the chemicals currently used to prepare commercial synthetic phenol–formaldehyde (PF) resins by either the novolac or resoles process.[1] PF resin is applied in diverse applications, including gluing metals, wood, plastics, paper and rubber with reasonable cost and mechanical characteristics.[2] Phenolic resins are synthesized globally in large volumes (5 million tons per year), and their growth is related to the gross national product (GNP) growth of countries.[2] Both phenol and formaldehyde are considered environmentally unfavorable chemicals and associated with several health issues by the Environmental Protection Agency (EPA). The European Chemical Agency (ECHA) has also classified both phenol and formaldehyde as mutagenic, carcinogenic, and reprotoxic chemicals. Formaldehyde is also used in some other resins in addition to the phenol–formaldehyde resin, such as urea–formaldehyde and melamine–formaldehyde resins that are produced in large volumes and used as wood adhesive or mineral fiber binders. Although formaldehyde has a huge market in resin applications, it is associated with environmental issues along with health concerns and is classified as one of the human carcinogenic chemicals by the World Health Organization (WHO) and US Occupational Safety and Health Administration (OSHA).[3]

Renewable raw materials, including cashew nut shell oil, tannins, bio-oil, and furfural, are used to replace or substitute for the unfavorable phenol.[4] Besides these renewable chemicals, tung oil and linseed oil are also used in limited amounts to substitute for phenol. Emerging biorefinery technologies are gaining much attention to produce and fulfill the market demand by generating renewable and sustainable chemicals, materials, fuels, and polymers. Among them, lignin from the biorefinery process and pulp industries still mostly exists in a waste solid stream that is currently burned to generate energy except for partially recovering certain chemicals.

Cellulose, hemicellulose and lignin as substantial fractions of lignocellulosic biomass represent the utmost sustainable and renewable candidates that can be processed to replace or substitute for petroleum-derived fuels, chemicals, materials, and polymers.[5–7] Lignin represents around one-third of the known structural biopolymers in lignocellulosic biomass (dry weight), and its structure justifies a wide range of modifications that involve the functionalization on hydroxyl, carbonyl groups, or phenolic rings (*i.e.*, *p*-coumeryl, coniferyl and sinapyl alcohols). Within the last two decades, lignin has been constantly studied for the production of different types of high-value, low-volume market or niche-market products, including carbon fibers and lignin-based adhesives.[8,9] Over

Department of Wood Technology and Wood-based Composites, Georg-August-University of Göttingen, 37077 Göttingen, Germany.
E-mail: kai.zhang@uni-goettingen.de

†Electronic supplementary information (ESI) available. See DOI: 10.1039/d2gc00014h

This journal is © The Royal Society of Chemistry 2022

Open Access Article. Published on 25 February 2022. Downloaded on 1/23/2026 6:06:52 PM.
This article is licensed under a Creative Commons Attribution-NonCommercial 3.0 Unported Licence.

the past few decades, lignin has been used as a partial or full (100%) replacement for phenol in PF adhesives.[4] For example, lignin-based phenolic oil was used to partially (20–50 wt%) replace phenol in the PF resins,[10] while Kraft lignin could even substitute for phenol at slightly higher quantities of 65 wt% in lignin–PF resins as adhesives.[11] In addition to these lignin types, glyoxalated lignin, silver–lignin nanoparticles, and lignin–epoxy hybrid nanoparticles were also used for lignin-based adhesives to substitute for phenol.[12–14]

In addition to phenol, the replacement or substitution of formaldehyde with less toxic, less volatile and biobased compounds can add further positive advantages over workers' health risks and environmental issues caused by chronic exposure to formaldehyde during the resin manufacturing process.[15,16] An alternative to formaldehyde will substantially impact its large consumer market of phenolic resins. To date, furfural, 5-hydroxymethyl furfural, terephthalaldehyde, succinic anhydride, glyoxal and citric acid as renewable and partially or fully alternative chemicals for formaldehyde have been applied to synthesize phenolic resins.[5,17–20] In particular, the full replacement of phenol by lignin will allow the development of totally novel adhesives with new ingredients. For instance, acrylic acid (AA) has been used with chitosan, polypropylene, and other substrates to prepare acrylic adhesives for pressure-sensitive and cell culture applications.[5,21,22] Such acrylic adhesives show advantages such as fewer human health hazards and are associated with fewer environmental issues relative to formaldehyde-based adhesives.

Herein, we developed a new protocol to overcome the limitations of phenol/formaldehyde-based resins using a lignin/AA-based adhesive with a high yield (Fig. 1A and B). This protocol involves the synergistic role of lignin, AA, and dimethylformamide (DMF) to form a versatile amphiphilic biobased adhesive that showed strong mechanical performances over a variety of adherents, including glass (G), stainless steel, (SS) aluminum (Al), polyvinyl chloride (PVC), polycarbonates (PC), and wood. Moreover, the functionalization of side chains, aryl ring, hydroxyl (1° or 2°) groups or phenolic hydroxyl groups of lignin with AA and DMF, is affirmed by FT-IR and NMR spectroscopy including one-dimensional (1D) $^{13}C/^{31}P$ spectroscopy and two-dimensional (2D) correlation spectroscopy as ^{13}C–^{1}H heteronuclear single quantum coherence (HSQC) and ^{13}N–^{1}H heteronuclear multiple bond correlation (HMBC). Substantially high storage and loss moduli of adhesive samples relative to polyvinyl alcohol (PVA), as a reference, were measured using dynamic mechanical thermal analysis (DMTA) over a range of conditions, including temperature, relative humidity, time, and frequency. The lignin-based adhesive showed excellent physical-mechanical properties after immersing adherent–adhesive samples in neutral, acidic (pH 3.08) and basic (pH 10.22) media. The lignin-based adhesive also demonstrated high bond strength, excellent stability during the weathering test (>64 d) and was able to hold 2.0×10^5 times its own weight without failure even after 94 d. A strong correlation was found between the polar component of surface free energy (SFE) and internal bond strength with R^2 values 0.98 and 0.96 over various substrates.

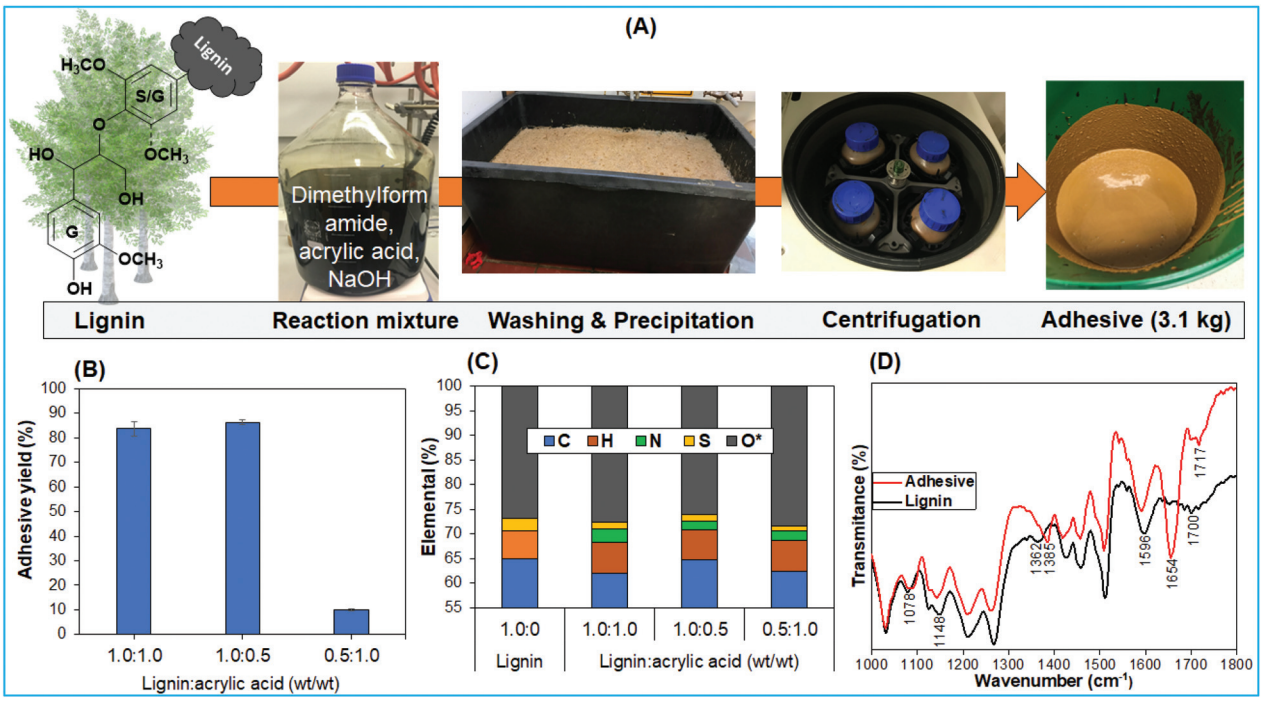

Fig. 1 Preparation of the lignin-based universal adhesive. (A) Schematic representation of the synthesis of lignin-based adhesives, the inset shows the photographs of intermediate steps (washing, precipitation and centrifugation) of the adhesive with lignin : acrylic acid of 1.0 : 1.0 (wt/wt). (B) Yields of adhesives, (C) The elemental composition of lignin and lignin-based adhesives (*O = 100 – (C + H + N + S)), and (D) FT-IR spectra of lignin and adhesive. The adhesive in (D) refers to the combination with lignin : acrylic acid of 1.0 : 1.0 wt/wt.

Open Access Article. Published on 25 February 2022. Downloaded on 1/23/2026 6:06:52 PM.
This article is licensed under a Creative Commons Attribution-NonCommercial 3.0 Unported Licence.

Results and discussion

Synthesis and characterization of the lignin-based universal adhesive

The lignin-based universal adhesive was synthesized using lignin and AA in DMF under basic medium, and the obtained yields are shown in Fig. 1B. Three different weight ratios of lignin and AA of 1.0 : 1.0, 1.0 : 0.5, and 0.5 : 1.0 with constant solid-to-liquid ratios (10 wt%, lignin wt/vol of DMF, except later specifically noted (20 wt%)), were used. Highly similar yields of 84% and 86% were obtained using weight ratios of lignin and AA at 1.0 : 1.0 and 1.0 : 0.5, respectively. Substantial differences of the contents of elements C, H, N, S, and O, particularly nitrogen, were measured (Fig. 1C). In comparison, the yield for the 0.5 : 1.0 (wt/wt) lignin : AA ratio was low, which could be explained based on the high solubility of lignin or modified lignin in DMF and due to the potential washing out during the purification steps. Additional washing of adhesives with aqueous solutions should also have contributed to decreasing the sulfur content (Fig. 1C).[23] Low sulfur content is advantageous as otherwise it can lead to odor issues along with a yellowish color in the final products.[24] The presence of nitrogen in lignin-based adhesives affirmed the lignin-functionalization with the involvement of DMF, which is also validated by the appearance of new peaks at 1654 cm^{-1} for amide and 1385 cm^{-1} for $-C(CH_3)_2$ groups in the FT-IR spectrum (Fig. 1D).[25] These modifications of the lignin backbone further induced a lower glass transition temperature of the adhesives relative to lignin (Fig. S1A†). The lower glass transition temperature of the lignin-based adhesive can support the crosslinking of lignin.[26] The functionalization or crosslinking of lignin to the lignin-based adhesive is also validated by thermogravimetric analysis (Fig. S1B†), as the crosslinked functionalities of the adhesive started to degrade at a lower temperature relative to those in lignin.[27]

NMR characterization of lignin and lignin-based universal adhesive

To underpin the FT-IR, DSC, and TGA analysis, the ^{13}C NMR spectra of both lignin and lignin-based universal adhesive (lignin : acrylic acid of 1.0 : 1.0 wt/wt, used for NMR) were recorded, and significant numbers of new peaks were observed in the lignin-based adhesive (Fig. 2A). A new chemical shift for the $-N(\mathbf{C}H_3)_2$ peak is observed at 43.21 ppm and can be validated from the moieties of DMF that is used to solubilize and functionalize lignin. Similarly, the peaks at 55.57 and 162.30 ppm for the carbon atoms in $Ar-\mathbf{C}H_2-$ and $R-(\mathbf{C}O)-N(CH_3)_2$ groups are also attributed to lignin functionalization by DMF. The presence of chemical shift data for these peaks is consistent with the results for lignin functionalization reported elsewhere.[28] Additionally, a few more extra peaks emerged at 130.40 and 167.40 ppm for the carbon atoms of $RO(CO)\mathbf{C}H-CH-$ and $RO(\mathbf{C}O)CH-CH-$ moieties, respectively. These carbon atoms in the lignin-based adhesive should plausibly be derived from AA for the synergistic reaction, whereas the chemical shift data for AA matched with the previous reports elsewhere.[29] Moreover, to validate the functionalization of lignin by DMF and AA in the lignin-based adhesive, $^{13}C-^{1}H$ correlation 2D-HSQC NMR spectra were recorded (Fig. 2B). New signals in the aliphatic and aromatic regions are assigned to the introduced $R-N(\mathbf{C}H_3)_2$ and $RO(CO)\mathbf{C}H-\mathbf{C}H-$ groups, comparing the spectra of lignin and the adhesive.[29] The $^{15}N-^{1}H$ correlation 2D-HMBC NMR spectrum of the lignin-based adhesive was also recorded to validate the functionalization of lignin by DMF (Fig. 2C). Interestingly, two new signals at 175.59/7.95 ppm and 175.59/2.75 ppm are assigned to the same nitrogen functionality with two different types of proton environments that are aromatic and aliphatic protons, respectively.[30] To find out the role of lignin hydroxyl (1°, 2° or phenolic hydroxyl) groups in the lignin functionalization to the lignin-based adhesive, ^{31}P NMR of both lignin and lignin-based adhesive samples were recorded, and the peak assignment was done according to previous reports.[31] The measurement of high-intensity peaks for carboxylic groups along with the condensed phenolic hydroxyl groups validated the modification of the lignin backbone (Fig. 2D). Fig. 2E shows the likely chemical structure of modified lignin, guaiacyl moiety, and various types of linkages in lignin-derived units.

Correlating lignin and adhesive properties: functional groups, linkages, and molar mass

Several notable trends were identified between the lignin and the lignin-based universal adhesive (Fig. 3), so that properties can be linked to potential suitability of the adhesive. The $^{13}C-^{1}H$ correlation 2D-HSQC NMR spectra of both lignin and lignin-based adhesive samples were used to measure the relative abundance of major linkages namely β-O-4, β-β, and β-5 linkages (Fig. 3A).[32] The lignin-based adhesive is characterized by the slightly decreased amount of (~7.1%) β-O-4 linkages compared to lignin that can plausibly be explained due to the susceptibility of lignin conversion under basic medium.[33] Moreover, the partial depolymerization of lignin to lower molar mass is also consistent with the generation of slightly higher amounts of phenolic hydroxyl groups (condensed-OH, *p*-coumeryl (H-OH), coniferyl (G-OH), and sinapyl (S-OH) alcohols) in the lignin-based adhesive (Fig. 3B and C). Moreover, the total hydroxyl (1°, 2°, and phenolic) contents were found to be slightly higher in adhesives than in pristine lignin (Fig. S2†). This measurement is consistent with the results from previous reports of lignin utilization in higher yields of hydroxyl products.[34] Moreover, the cleavage of β-O-4 linkages should have resulted in the formation of new phenolic hydroxyl groups (Fig. 3B and C), and therefore also the adhesives of lower molar mass (Fig. 3D).[35] These data for linkages, hydroxyl groups and molar mass added further correlations during the modification of lignin for adhesives.[36] In particular, the development of diverse hydroxyl groups and linkages shows specific characteristics of the synergistic reactions between lignin, AA and DMF compared to previous reports.[5,37]

Dynamic mechanical thermal analysis of lignin-based universal adhesive

Mechanical properties such as storage modulus, loss modulus, and tan delta of lignin-based adhesives with different lignin to

 This journal is © The Royal Society of Chemistry 2022

Open Access Article. Published on 25 February 2022. Downloaded on 1/23/2026 6:06:52 PM.
This article is licensed under a Creative Commons Attribution-NonCommercial 3.0 Unported Licence.

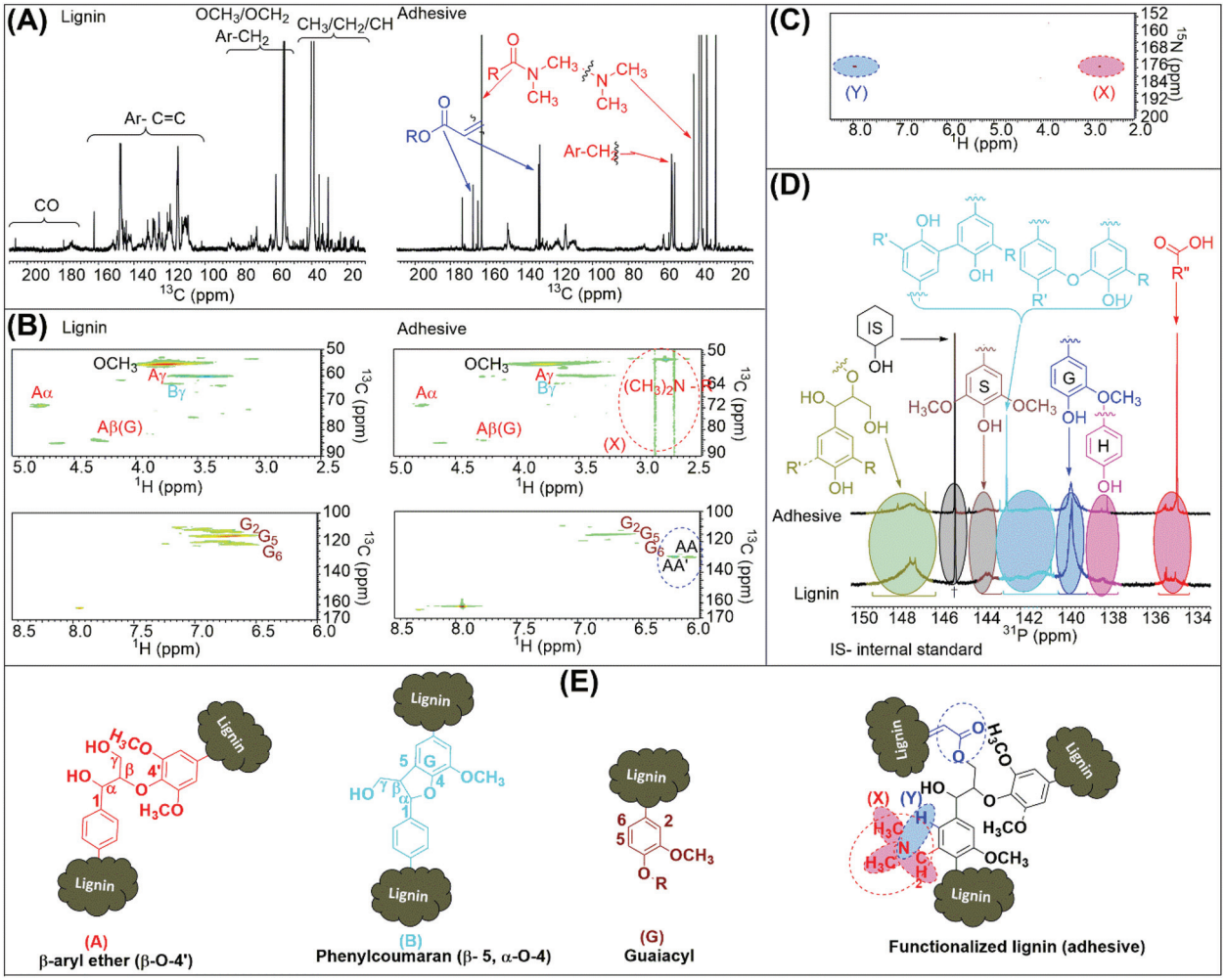

Fig. 2 Anticipated chemical structures of lignin/lignin-based universal adhesive. (A) ^{13}C NMR spectra of lignin and adhesive, (B) ^{13}C–^{1}H correlation 2D-HSQC NMR spectra of lignin and adhesive, (C) ^{15}N–^{1}H correlation 2D-HMBC NMR spectrum of adhesive, (D) ^{31}P NMR spectra of lignin and adhesive, and (E) the anticipated structure of various linkages, moieties in lignin and modified lignin. X and Y represent ^{15}N–^{1}H correlation 2D-HMBC signals for N–H (aliphatic proton) and N–H (aromatic proton) respectively. AA and AA′ represent the HSQC signals for modified acrylic acid in lignin-based universal adhesive. The adhesive with lignin : acrylic acid of 1.0 : 1.0 (wt/wt) was used for NMR.

AA ratios, and PVA, were investigated by DMTA to understand the effects of crosslinking by DMF and AA to lignin. The DMTA of adhesive samples was investigated over time (t), temperature (T), frequency (f) and relative humidity (RH) (Fig. 4 and S3, S4†). Physiological properties, such as the storage modulus of adhesive materials, generally change over the applied temperature, while materials mostly stay as a glassy/crystalline state and transform to rubbery/melted state at a higher temperature.[38] According to DMTA measurements, the storage modulus and tan delta values of our adhesives are stable for more than 4 h at 25 °C, 30% RH with a frequency of 10 Hz (Fig. 4A). This is anticipated by the heterogeneous nature of lignin with various types of moieties and linkages, which can induce the local relaxation and dynamically responsive states of lignin-based adhesives.[39] DMTA data of lignin-based adhesive with the lignin : AA ratio of 1.0 : 0.5 (wt/wt) show higher storage modulus (35.4 GPa) than the 21.2 GPa for the adhesive with lignin : AA ratio of 1.0 : 1.0 (wt/wt). This difference could plausibly be explained by different extents of functionalization by AA. A higher amount of AA led to stronger cleavage of the lignin backbone (Fig. 1C, 2B and D).

The storage modulus of both lignin-based adhesives and PVA as reference (Fig. S5†) substantially increases over the tested frequency (0.1 to 100 Hz) at 25 °C and 30% RH (Fig. 4B), whereas the tan delta values increase up to a certain higher frequency and then remain almost constant. The substantial increment of storage, tan delta, and loss modulus implied the crosslinking and densification of lignin-based adhesive over tested frequencies that further strengthen the inter and intra linkages in the adhesive.[40] Lignin associates with both the hydrophobic (aryl moiety) and hydrophilic (alkyl alcohols side-chains) groups which implied the formation of either-side chain cross-linkages or aryl networks.[41] Fig. 4C demonstrates the impact of RH on the mechanical properties of lignin-based

Open Access Article. Published on 25 February 2022. Downloaded on 1/23/2026 6:06:52 PM.
This article is licensed under a Creative Commons Attribution-NonCommercial 3.0 Unported Licence.

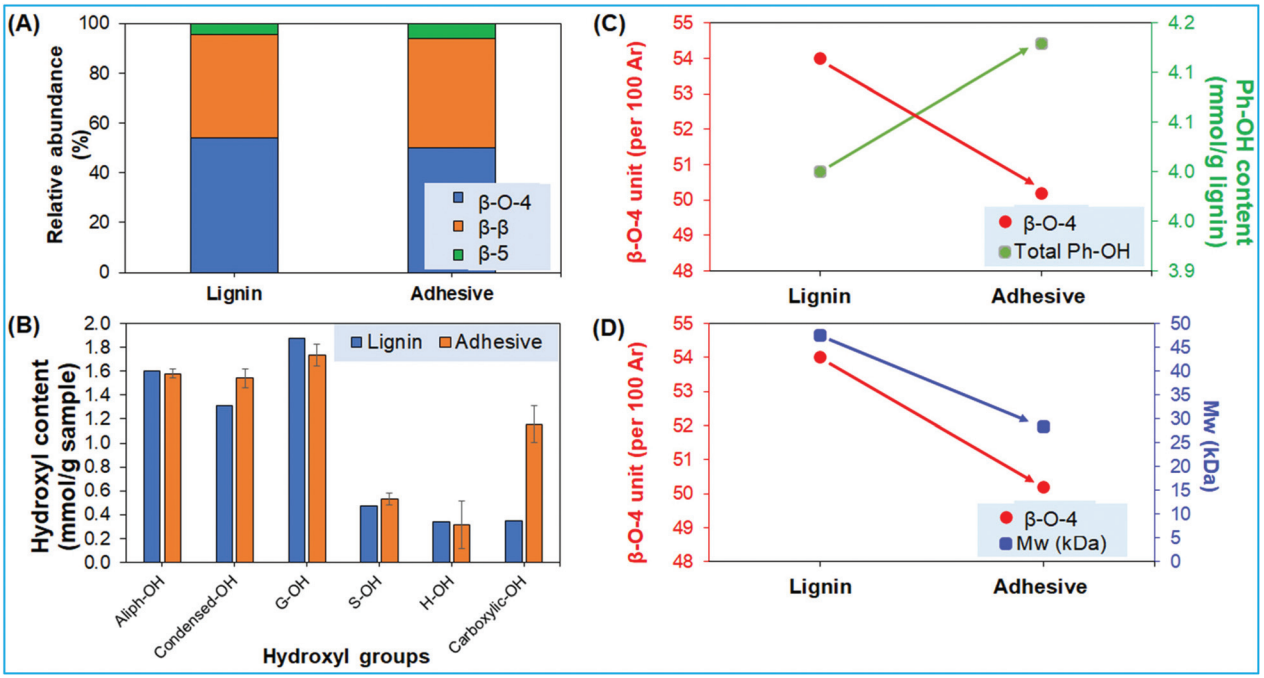

Fig. 3 The amounts of various major linkages and hydroxyl groups in lignin and lignin-based universal adhesive. (A) Relative abundance of major linkages in lignin and adhesive calculated by $^{13}C–^{1}H$ correlation 2D-HSQC NMR, (B) contents of hydroxyl groups in lignin and adhesive calculated by ^{31}P NMR, (whereas H represents *p*-coumaryl, G coniferyl and S sinapyl alcohols), (C) correlation between the content of β-O-4 linkage and phenolic hydroxyl groups, and (D) correlation between weight-average molar mass and the amount of β-O-4 linkage. The adhesive obtained with lignin : acrylic acid of 1.0 : 1.0 (wt/wt) was used.

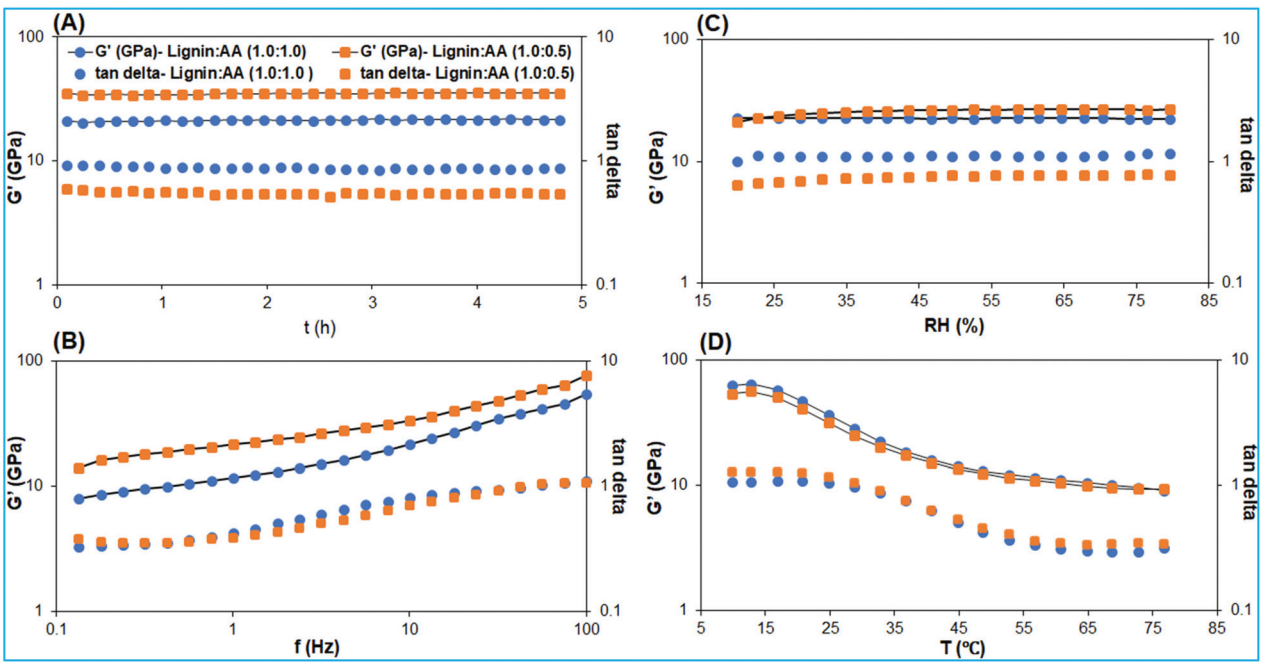

Fig. 4 Mechanical analysis of lignin-based universal adhesive. DMTA for storage modulus (*G'*) of adhesive (with lignin : AA ratios of 1.0 : 1.0 and 1.0 : 0.5, wt/wt). (A) Time sweep at 25 °C and 30% RH with a frequency of 10 Hz, (B) frequency sweep at 25 °C and 30% RH, (C) relative humidity (RH) sweep at 25 °C with a frequency of 10 Hz, and (D) temperature sweep at 30% RH with a frequency of 10 Hz and temperature increase rate of 2 K min^{-1}.

 This journal is © The Royal Society of Chemistry 2022

Open Access Article. Published on 25 February 2022. Downloaded on 1/23/2026 6:06:52 PM.
This article is licensed under a Creative Commons Attribution-NonCommercial 3.0 Unported Licence.

adhesives. The storage modulus of the adhesive (lignin : AA of 1.0 : 0.5, wt/wt) slightly increased from 21.1 GPa to 26.7 GPa, as the RH increased from 19.8% to 79.6%, whereas the storage modulus of PVA slightly decreased from 20.9 GPa to 19.1 GPa as RH increases from 22.7% to 79.6%, respectively (Fig. S4†). The slight increment in the storage modulus of the lignin-based adhesive and PVA could plausibly be explained due to different functionalities of lignin as dense phenolic and side-chain cross-linkages.[6,42] Storage moduli and tan delta of both lignin-based adhesives and PVA as adhesive were substantially high and stable at a low temperature (~16.0 °C). At a higher temperature of 48.8 °C, they decreased significantly to an extent of ~75% and decreased further at ~80 °C (Fig. 4D). We anticipate that the plural functionalities and aryl moieties of the lignin-based material over the applied temperatures can exhibit phase changes from crystalline/glassy to rubbery/melted, and represented substantially decreased storage modulus and tan delta at raised temperatures.[43] Similar to the storage modulus, the loss modulus trend could depict the more elastic polymeric nature of the lignin-based adhesive (Fig. S3†).[44] The good mechanical stability of the lignin-based adhesive under the applied static and dynamic loading represents the sufficient stiffness and robustness of adhesives without any fatigue for the long term.

Internal bond strength and surface free energy of the lignin-based universal adhesive

The adhesion property of the lignin-based universal adhesive depends on the adherent–adhesive internal bonding chains.[45] The internal bond strength (IBS) of lignin-based adhesives with a lignin : AA ratio of 1.0 : 1.0 (wt/wt) and PVA-based adhesives on different types of adherents, including glass (G), aluminum (Al), stainless steel (SS), and polycarbonate (PC), is shown in Fig. 5A (Table S1 and Fig. S5,† for more details about the adherent dimensions). Interestingly, PC represents the maximum IBS relative to the other tested adherents (Fig. 5A). Comparing the adhesive property over Al, the adhesive with the lignin : AA ratio of 1.0 : 1.0 wt/wt showed a significantly higher internal bond strength (~35%) than the adhesive with the lignin : AA ratio of 1.0 : 0.5 wt/wt. It can plausibly be anticipated due to more intensive functionalization and crosslinking of the lignin backbone (Fig. 1C, and 2A–D).[13] Inconsistent with the DMTA analysis of the adhesive and PVA (Fig. 5A and Fig. S5†), statistically slightly higher IBS (186.25 kPa) is measured for the Al–lignin-based adhesive (1.0 : 1.0 wt/wt) compared to Al-PVA (180.0 kPa). Our lignin-based adhesives exhibited high bonding strengths for a variety of substrates including glass, metal and plastics, in comparison with currently used adhesives, *e.g.* acrylate, esters, sugars and amino acids that are generally used for limited substrates.[46] The highest IBS of the lignin-based adhesive was characterized on PC, which is consistent with the substantial change in surface free energy (SFE) of the PC (control) and PC-S (S represents the material coated with the adhesive, lignin : AA ratio of 1.0 : 1.0, wt/wt) (Fig. 5B). In general, the dispersion SFE (hydrophilicity) of adhesive materials (G-S, Al-S, SS-S, and PC-S) increases except for the PVC-S, whereas the polar SFE (hydrophobicity) consistently also increases (except G-S). The substantial difference in polar SFE of PC (with and without adhesive coated) was measured (Fig. 5B), which can validate the higher IBS of PC with the adhesive. In general, polar interaction played a substantial role in the IBS of adherent–adhesive.[47] The hydrophilicity and hydrophobicity for lignin-based adhesive over the various types of adherents were determined using static water contact angle (CA) measurement (Fig. 5B). The CA of G-S and PVC-S samples increases in a similar manner as those of substrates without adhesive, whereas a negative trend measures for Al-S, SS-S, and PC-S (Fig. 5B). This can plausibly be validated due to the orientation of phenolic moieties and side chains of the lignin-based adhesive.[48] Moreover, the G-S, Al-S, and PC-S samples showed a strong correlation between the SFE polar and IBS (Fig. 5C), which are consistent with the results of the previous reports elsewhere.[49] An excellent correlation fits for SFE polar and IBS of G, Al, and PC materials with the lignin-based adhesive (lignin : AA of 1.0 : 1.0, wt/wt), which are plotted with R^2 of 0.98 and 0.96, respectively. These correlations concluded the strong interactions between the G, Al, and PC material with the lignin-based adhesive.

Physical-mechanical weight and weathering tests of the lignin-based universal adhesive

In addition to the aforementioned excellent mechanical properties, long-term durability, environmental sustainability, and stability in different media are also important for a wide range of potential applications of the adhesives.[45] To demonstrate the interfacial adhesive strength and durability of the lignin-based adhesive (lignin : acrylic acid of 1.0 : 1.0, wt/wt) over G, PC, PVC, and wood (Fig. 6), a rectangular surface was glued with the adhesive and subjected to vertical and horizontal physical-mechanical weight testing (Tables S2, S3 and Fig. S5, S6 and S7,† for more details on material dimensions and glued areas). Thereafter, samples were dried at 105 ± 2 °C for 2 h. The PC and PVC glued with adhesive were able to vertically hold 1.5×10^5 times their own weight without failure for ~10 min (tested time). The same glued samples were immersed in DI water for 30 min at ambient temperature (Fig. 6B) and the vertical mechanical weight performance was measured. The samples were able to hold 1.0×10^5 times their own weight without failure for ~10 min (tested time). These samples after DI water treatment were further immersed in an aqueous acidic solution (pH 3.08, using 72% H_2SO_4) for 30 min at ambient temperature (Fig. 6C), before their mechanical performance was examined. The samples successfully held 1.0×10^5 times their own weight without failure for ~10 min (tested time). The samples after acidic treatment were then immersed in an aqueous basic solution (pH 10.22, NaOH) for 30 min at ambient temperature, and the mechanical weight holding performance was examined by applying 1.5×10^5 times weight of adhesive weight on the same day and after 30 d (stored under ambient conditions) (Fig. 6D and E). As shown with vertical mechanical weight testing of PC and PVC glued

Open Access Article. Published on 25 February 2022. Downloaded on 1/23/2026 6:06:52 PM.
This article is licensed under a Creative Commons Attribution-NonCommercial 3.0 Unported Licence.

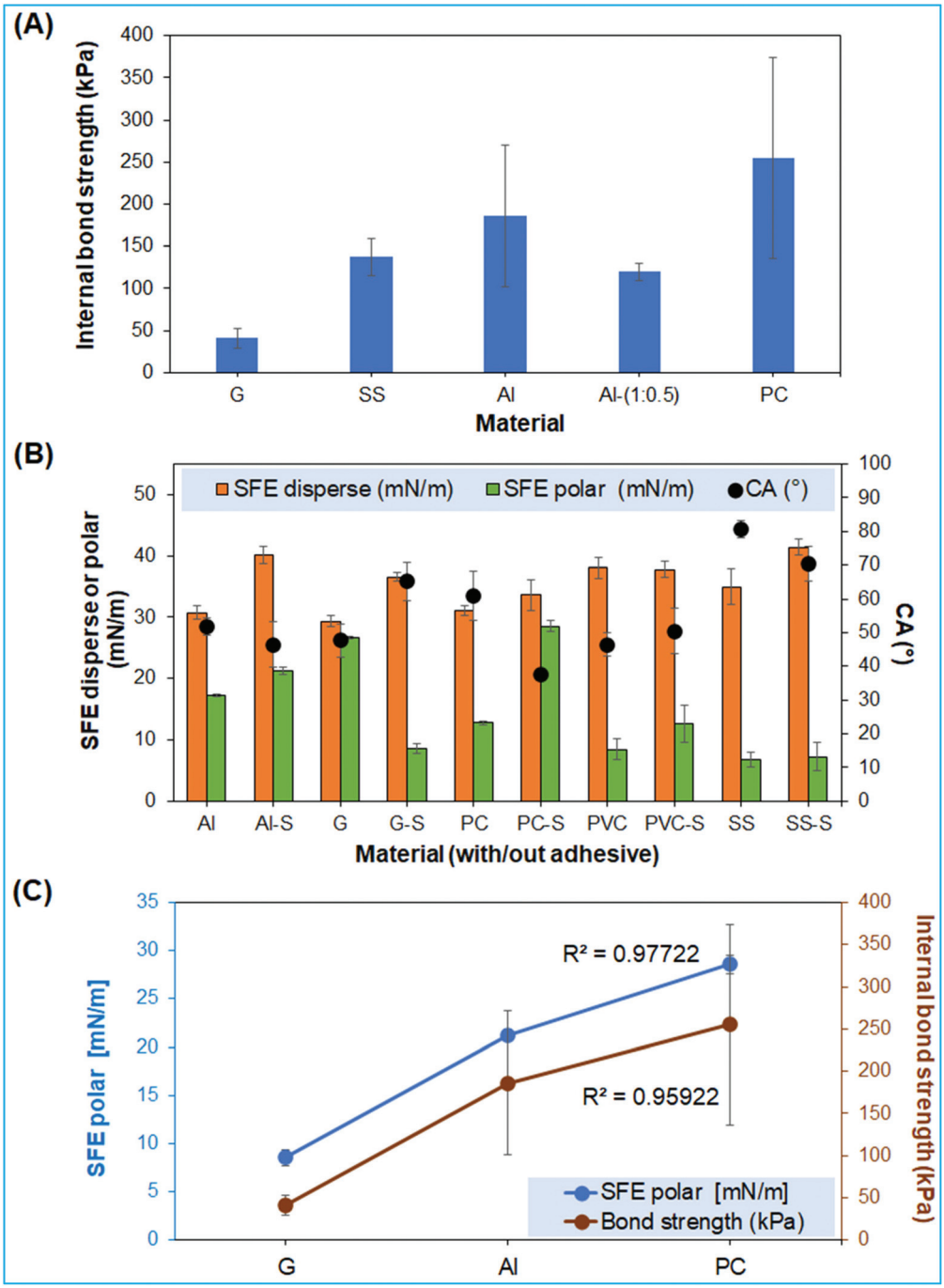

Fig. 5 Internal bond strength and surface properties of the universal adhesive. (A) Internal bond strength of adhesive, reference over glass (G), stainless steel (SS), aluminum (Al), and polycarbonate (PC), (B) cumulative polar and dispersed components of SFE, and static contact angle (°) (S indicates adherents with adhesive), and (C) correlation between polar components of SFE and internal bond strength. The adhesive obtained with lignin : acrylic acid of 1.0 : 1.0 (wt/wt) was used in Fig. 5, unless notified.

samples, the lignin-based adhesive was highly stable under neutral, acidic, and basic media for more than 30 d.

The samples treated in basic solutions were then processed for the weathering test for 64 d (From September 13, 2021 to November 15, 2021, Göttingen, Germany). Samples displayed a similar holding performance of 1.5×10^5 times their own weight without failure (Fig. 6F). Therefore, the lignin-based universal adhesive (lignin : acrylic acid of 1.0 : 1.0, wt/wt), demonstrated environmental sustainability along with an excellent property to hold loading of a ratio of 1.5×10^5 its own weight for the long term. Glued samples as G, PC, PVC, and wood were used to measure the horizontal interfacial adherent–adhesive strength (Fig. 6G) (more details about the gap between two stands and stand height in Fig. S7†). The PVC

 This journal is © The Royal Society of Chemistry 2022

Open Access Article. Published on 25 February 2022. Downloaded on 1/23/2026 6:06:52 PM.
This article is licensed under a Creative Commons Attribution-NonCommercial 3.0 Unported Licence.

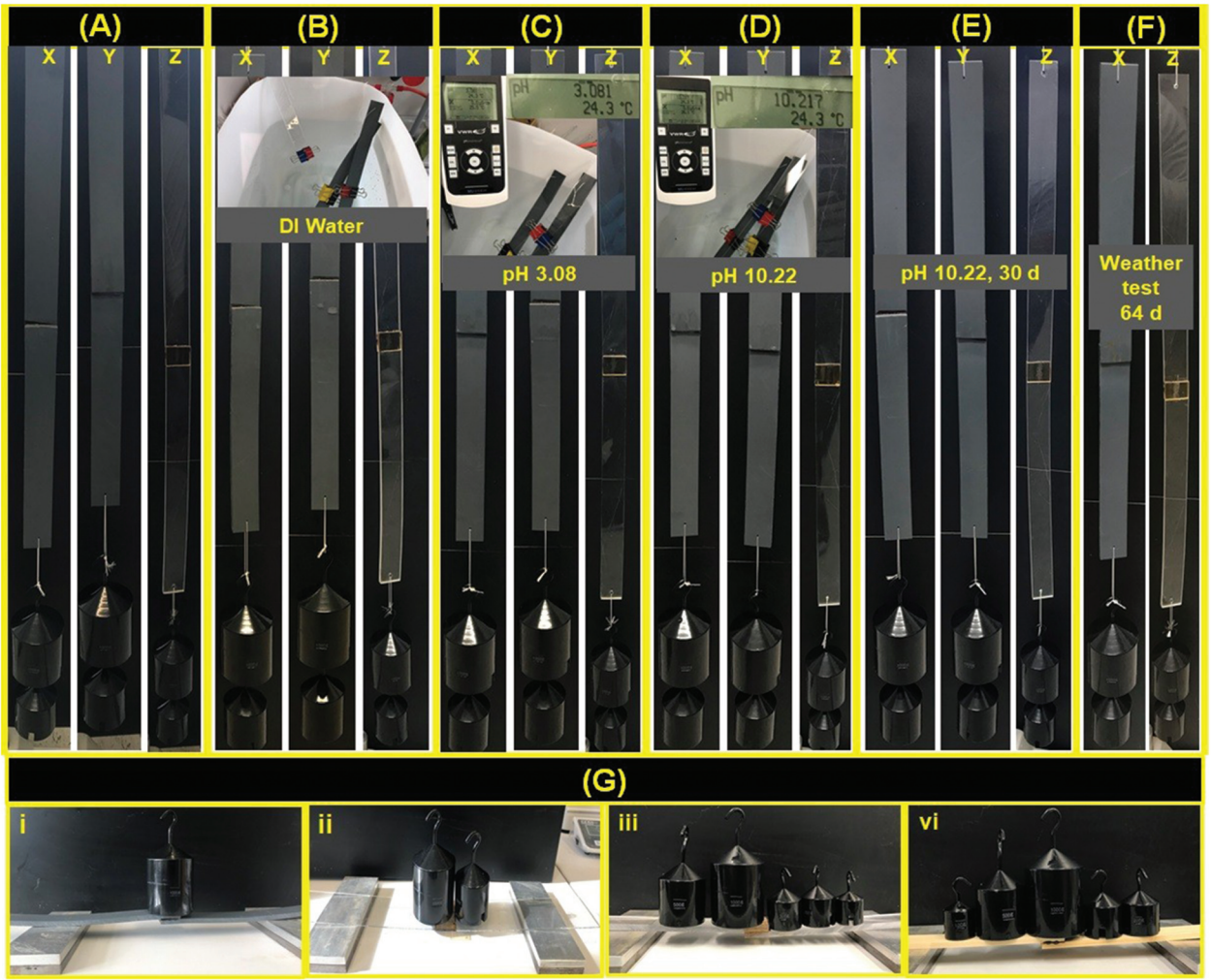

Fig. 6 Vertical physical-mechanical testing (1500 g) of adhesive on PVC (*x*: 2.5 cm^2 glued area and *y*: 5.0 cm^2 glued area) and PC (*z*: 5.0 cm^2 glued area) over various pH values and days (d). (A) Dried, (B) immersed in DI water for 30 min, (C) immersed in aqueous acidic 72% H_2SO_4 medium (pH 3.08) for 30 min, (D) immersed in aqueous basic NaOH medium (pH 10.22) for 30 min, (E) after 30 d ambient conditions, (F) weathering test for 64 d (total 94 d), and (G) horizontal mechanical testing (5.0 cm^2, except for glass with 10.0 cm^2 glued area), (i) PVC (1000 g), (ii) G (1500 g), (iii) PC (2000 g) and (iv) wood (2000 g). The adhesive obtained with lignin : acrylic acid of 1.0 : 1.0 (wt/wt) was used in Fig. 6.

and G glued samples were able to hold horizontally up to 1.0×10^5 times and 1.5×10^5 their own weight, respectively, whereas the PC and glued wood samples could hold 2.0×10^5 times their own weight without failure.

Conclusions

A green, sustainable, and biobased universal adhesive is investigated using lignin, DMF and AA in basic medium. The internal bond strength (IBS) of the lignin-based adhesive was measured over the various types of adherents (G, Al, SS and PC), and promising IBS is validated for the PC glued sample. The universal biobased adhesive is environmentally sustainable (64 d), and chemically stable towards acidic (pH 3.08), neutral and basic (pH 10.22) media. Following lignin functionalization using AA and DMF, the lignin-based adhesive was characterized using elemental analysis, FT-IR, 1D ^{13}C, ^{31}P, 2D ^{13}C–^{1}H HSQC and ^{15}N–^{1}H HMBC correlation NMR spectroscopy. Excellent dynamic mechanical properties were measured for the lignin-based adhesive on various substrates. Thus, we developed a synergistic facile synthesis method for a lignin-based universal adhesive that can be a route to replace the commercially widely used formaldehyde-based resins, and may bring the possibility of a potential solution for the environmental and health-related issues.

Experimental

Materials

UPM BioPivaTM 100 lignin was received as a gift for research from the UPM Biochemicals, Helsinki, Finland, and it was air-dried at ambient temperature for 24 h before use. Sodium

Open Access Article. Published on 25 February 2022. Downloaded on 1/23/2026 6:06:52 PM.
This article is licensed under a Creative Commons Attribution-NonCommercial 3.0 Unported Licence.

hydroxide was received from Sigma-Aldrich, Darmstadt, Germany. Dimethylformamide (99.8%), methanol (99.8%), ethanol (99.9%), and tetrahydrofuran (THF, 99.9%) were purchased from Th. Geyer GmbH. Dimethylsulfoxide-d_6 was purchased from Carl Roth GmbH. Acrylic acid (AA) stabilized with 200 ppm 4-methoxyphenol was purchased from Alfa Aesar, Germany. Chromium(III) acetylacetonate was purchased from Sigma-Aldrich, USA. Anhydrous dimethylformamide (99.8%) and anhydrous pyridine (99.8%) were purchased from Sigma Aldrich, Germany. 2-Chloro-4,4,5,5-tetramethyl-1,3,2-dioxaphospholane (95.0%) was purchased from Sigma Aldrich, India. Polyvinyl alcohol (PVA, 99+% hydrolyzed, $\overline{M_w}$: 89–98 kDa) was purchased from Sigma-Aldrich, Germany. Cyclohexanol (99.0%) was purchased from Sigma Aldrich, China. All the chemicals were used as received with any purification step.

Synthesis of lignin-based adhesive

Lignin (1.0 g, based on dried) was taken in a glass pressure tube (35 mL, or 120 mL for 3.0 g of sample, FengTecEx GmbH), and in that, 10 or 30 mL of DMF along with 100 or 300 mg of NaOH, was added. The reaction mixture was stirred using a stir bar (500 rpm) at room temperature (RT) for 1 h. Thereafter, AA (1.0 g or 3.0 g) was added to the same mixture and stirred further at ambient temperature for 24 h (total reaction time, 25 h). The obtained reaction mixture was processed for modification of lignin in a preheated oven at 105 ± 2 °C for 45 ± 0.2 h. After lignin modification, the mixture was allowed to cool at ambient temperature (cooling time ~20 min). DI water (50 mL or 150 mL) was added to wash the mixture, which was then processed for centrifugation (Universal 320, Hettich, Germany) at 4000 rpm for 10 min. The obtained semi-solid as a lignin-based universal adhesive, was semi-dried at ambient temperature for 24 ± 0.2 h, and yield was calculated using charged lignin as denominator thereafter drying the adhesive at 105 ± 2 °C, 4 h.

Adhesives with lignin : AA of 1.0 : 0.5 and 0.5 : 1.0 (wt/wt) were synthesized using the similar procedure as mentioned for the adhesive with lignin : AA of 1.0 : 1.0 (wt/wt), except for different amounts of AA and lignin. AA (0.5 g) and lignin (0.5) were used for the synthesis of adhesive (lignin : AA, 1.0 : 0.5) and adhesive (lignin : AA, 0.5 : 1.0), respectively. In addition, the adhesive with lignin : acrylic acid of 1.0 : 1.0 (w/w) was synthesized on a large scale (3.01 kg) for further applications (Fig. 1).

Polyvinyl alcohol (PVA) adhesive was synthesized by adding hot (~80 °C) DI water to PVA. The amount of water was selected based on the moisture contents (~80%) in the adhesive (lignin : AA, 1.0 : 1.0). The ratio (4 : 1 wt/wt) of water and PVA was taken in a glass vial (7.0 mL) with a PTFE cap liner to synthesize the PVA adhesive. The resulting mixture was placed in a preheated oven at 105 ± 2 °C for 2 h to polymerize the PVA. The synthesized PVA adhesive was used for analysis without any further modification.

Characterization

Fourier transform infrared (FT-IR). The functional groups in both lignin and lignin-based universal adhesive, were characterized by the ATR technique (ALPHA Bruker) using the OPUS 7.5 software. The spectra were recorded by applying the resolution 4 cm^{-1} with 32 phase resolutions. The sample scan time was 24 scans, and the data were saved from 4000 to 400 cm^{-1}. Prior to analysis, samples were dried at 105 ± 2 °C for 4 h, and stored in a glass vial with a PTFE cap liner.

Thermogravimetric analysis (TGA). Thermal degradation of samples was measured at TG 209 F1, NETZSCH, Germany. Approximately 10 mg of the sample was used to measure the thermal degradation with a heating rate of 20 K min^{-1} up to 800 °C in a N_2 atmosphere.

Differential scanning calorimetry (DSC). DSC analysis of samples was performed using DSC 200 F3, NETZSCH, Germany. Approximately 10 mg of the sample was heated to analyze the DSC with a heating rate of 10 K min^{-1} up to 300 °C in a N_2 atmosphere.

^{13}C and ^{13}C–^{1}H correlation 2D-HSQC NMR

The ^{13}C and ^{13}C–^{1}H heteronuclear single quantum correlation (HSQC) NMR spectra of lignin and lignin-based universal adhesive samples were measured using Brucker 500 MHz and 600 MHz instruments, respectively. The NMR sample was prepared with minor modifications using a report previously published elsewhere.[32] Approximately 100 mg (dried) of the sample and chromium(III) acetylacetonate (~2.0 mg) were taken in a glass vial. DMSO-d_6 (0.6 mL) was added in the same vial and the mixture was transferred for sonication for 10 min to facilitate solubilization. The completely soluble sample was transferred into an NMR tube and processed for the NMR spectra. The ^{13}C NMR spectra were recorded from −31.21 ppm to 230.30 ppm using 996.15 ms acquisition time (AQ) and with 203 receiver gain. The ^{13}C NMR tube was processed for ^{13}C–^{1}H correlation 2D-HSCQ NMR spectra at 600 MHz instruments, and analysis was performed with 600.25 MHz and 150.93 MHz applied frequency for ^{1}H and ^{13}C nuclei, respectively. The hsqcedetgpsisp2.3 current pulse program was applied. The ^{1}H and ^{13}C spectra were recorded from 0 to 15.2 ppm and from 0 to 220.0 ppm with an AQ of 112.64 and 7.71 ms, respectively. The semiquantitative relative abundance of linkages, including β-O-4, β-β, and β-5, was measured using the Bruker TopSpin 4.0.7 software. The peak assignments were done using the previous report elsewhere.[30]

^{15}N–^{1}H correlation 2D-HMBC NMR

A similar solution to that for the ^{13}C NMR spectra was prepared for ^{15}N–^{1}H correlation 2D-heteronuclear multiple bond correlation (HMBC). The HMBC analysis was performed using 500.25 MHz and 50.71 MHz for ^{1}H and ^{15}N nuclei, respectively. The hmbcgpndqf current pulse program was applied with an AQ of 204.80 ms and 67.32 ms for ^{1}H and ^{15}N nuclei, respectively. The applied receiver gain was 203.

^{31}P NMR for the determination of contents of hydroxyl groups

A Brucker 600 MHz instrument was used to measure the ^{31}P NMR spectra. The current pulse program, zgpg30 was applied with 128 scans. The analysis acquisition time was 1.013 ms

 This journal is © The Royal Society of Chemistry 2022

Open Access Article. Published on 25 February 2022. Downloaded on 1/23/2026 6:06:52 PM.
This article is licensed under a Creative Commons Attribution-NonCommercial 3.0 Unported Licence.

with 101 receiver gains. The spectra were recorded from −3.5 ppm to 196.1 ppm. The ^{31}P NMR sample was prepared with minor modifications using a report previously published elsewhere.[50] Approximately 40.0 mg of lignin (dried) or adhesive (dried) sample was dissolved in an anhydrous pyridine/deuterated chloroform mixture (325 μL, 1.6 : 1.0 v/v) and anhydrous DMF (300 μL). As an internal standard, cyclohexanol (100 μL, 22.0 mg mL^{-1}) in anhydrous pyridine/deuterated chloroform (1.6 : 1.0, v/v), was added. As a relaxation agent, chromium(III) acetylacetonate solution (50 μL, 5.6 mg mL^{-1}) in anhydrous pyridine/deuterated chloroform (1.6 : 1.0, v/v) was also added in the same tube. Ultimately, a phosphorylating reagent, 2-chloro-4,4,5,5-tetramethyl-1,3,2-dioxaphospholane (100 μL) was added, and sample processed for the ^{31}P NMR.

Dynamic mechanical thermal analysis (DMTA)

The DMTA measurement was performed using a DMA GABO EPLEXOR system (NETZSCH GABO Instruments GmbH) with a force sensor of 50.0 N. The applied static and dynamic force loads were 10.0 N (0.1% limit) and 5.0 N (0.05% limit), respectively. The applied contact force was 0.5 N. The soaking time for all samples was 300 s. Temperature sweep (10–80 °C) test was determined at 30% relative humidity (RH) with a frequency of 10.0 Hz and a temperature step rate of 2 K min^{-1}. The frequency sweep (0.1–100.0 Hz) test was determined at 25 °C, 30% RH with 8.0 steps per dec frequency increment. The RH (10%–80%) sweep test was carried out at 25 °C, with a frequency of 10.0 Hz. Time sweep (0–5 h) test was performed at 25 °C and 30% RH with a frequency of 10.0 Hz. Prior to analysis, the adhesive samples were glued between two glass slides (Fig. S2E†), and dried at 105 ± 2 °C for 2 h. The glued samples with different material dimensions of 10.0 mm × 0.005 mm for adhesive with lignin : AA of 1.0 : 1.0 (wt/wt), 9.0 mm × 0.001 mm for adhesive with lignin : AA of 1.0 : 0.5 (wt/wt), and 8.0 mm × 0.005 mm for PVA were used for DMTA. Moreover, the dimension correction factor for different samples was applied. The DMTA testing of adhesive with lignin : AA of 1.0 : 1.0 wt/wt) was done in replicate, and the average of replicates (temperature, time, frequency, and humidity sweep tests) is shown in Fig. 4 and S3, S4.†

Contact angle and surface free energy

The contact angle (CA) and surface free energy (SFE, polar and dispersion energy) of with/without adhesive samples were determined using OWRK, an SFE model. The water droplet on the samples was recorded by a video camera. The contact angle was measured using the image analysis software. Water and diiodomethane were employed as liquids with different polarities to measure the SFE. A minimum of 3–6 surface points per sample with 30 to 60 data sets were taken to determine the CA and SFE, and their average is presented. The plane surface of glass (G), polyvinyl chloride (PVC), stainless steel (SS), polycarbonate (PC), and aluminum (Al), and their glued samples (lignin : acrylic acid (AA), 1.0 : 1.0 wt/wt) were used for the CA and SFE determination. Prior to analysis, very fine adhesive layers (glued thickness 0.031 ± 0.007 mm) were added over the materials and dried at 105 ± 2 °C for 2 h.

Gel permeation chromatography

GPC was performed on an Agilent Technology 1260 Infinity system equipped with an isocratic pump and an autosampler. A refractive index (RI)-detector was used for the analysis. The GRAM columns with a guard column 8 × 50 mm of 10 μ and three separation columns (PSS Gram 1× 30 Å, 2× 1000 Å, all three of 10 μ), were used for the determination of molar masses. The flow rate was 0.8 mL min^{-1} and temperature 45 °C with dimethylacetamide (DMAc) as solvent was used. The sample concentration was 1.0 g per liter, and the injected volume was 50 μL. Calibration polystyrene standards were from 370 g mol^{-1} to 1.2 million g mol^{-1}.

Internal bond strength test

The internal bond strength (IBS) of the adhesives (lignin : AA, 1.0 : 1.0 wt/wt and lignin : AA, 1.0 : 0.5 wt/wt) and PVA over the G, SS, PC, and Al, was measured using DIN EN 1607 (2013) (Table S1, and Fig. S5,† for more details of material dimensions).[51] Prior to the IBS measurement, the adhesive samples were dried at 105 ± 2 °C for 2 h. Different substrates such as G, SS, PC, and Al were used for IBS samples (50 mm × 50 mm, except Al) and were glued between two Al yokes (for Al-IBS, the sample was used directly without fixing with yokes). The fixed samples were tested using a universal testing device (Zwick Roell, Ulm, Germany).

Physical mechanical testing

Vertical or horizontal physical-mechanical testing of the adhesive was done over various materials, including G, PVC, PC, and pine wood (approximately 20 years old) (Tables S2, S3 and Fig. S6, S7,† for more details of material dimensions). Approximately 10 mg (dried) of adhesive (lignin : AA, 1.0 : 1.0 wt/wt) was applied to laminate the materials (except wood ~100 mg, dried basis, due to porosity) between two layers, and the laminated samples were dried at 105 ± 2 °C for 2 h.

Weathering test

The PC, and PVC glued (lignin : AA, 1.0 : 1.0 wt/wt) samples were tied with a cable tie over a wire net and tilted with 45° (Table S2 and Fig. S6,† for more details of material dimensions). The net height from the ground was ~1.2 m. The samples were processed for weathering test from September 13, 2021 to November 15, 2021, at the test field of Georg-August University of Göttingen, Göttingen, Germany.

Conflicts of interest

There are no conflicts to declare.

Open Access Article. Published on 25 February 2022. Downloaded on 1/23/2026 6:06:52 PM.
This article is licensed under a Creative Commons Attribution-NonCommercial 3.0 Unported Licence.

Acknowledgements

KZ would like to thank the German Research Foundation (DFG) and Lower Saxony Ministry of Science and Culture for the project INST186/1281-1/FUGG. KZ would also like to thank the German Research Foundation GZ: 546/3-1 for the financial support and the Georg-August University of Göttingen for the Department Start-up funding. We thank Sandra Lotze (Institute for Physical Chemistry, Georg-August University of Göttingen, Göttingen, Germany) for performing the GPC analysis and also Siyuan Liu (Wood Technology and Wood-based Composites, Georg-August University of Göttingen, Göttingen, Germany) for helping with the DMTA analysis. We thank Jean Lawrence Tene Tayo for testing the internal bond strength. We also thank Mirko Küppers and Lukas Becker for helping to fix the samples for the weathering test.

Notes and references

1 K. J. Saunders, *Phenol-Formaldehyde Polymers*, Springer Netherlands, Dordrecht, 2 edn, 1988.
2 L. Pilato, *Phenolic Resins: A Century of Progress*, Springer, 2010.
3 W. D. Kerns, K. L. Pavkov, D. J. Donofrio, E. J. Gralla and J. A. Swenberg, *Cancer Res.*, 1983, **43**, 4382–4392.
4 A. Effendi, H. Gerhauser and A. V. Bridgwater, *Renewable Sustainable Energy Rev.*, 2008, **12**, 2092–2116.
5 L. A. Heinrich, *Green Chem.*, 2019, **21**, 1866–1888.
6 B. M. Upton and A. M. Kasko, *Chem. Rev.*, 2016, **116**, 2275–2306.
7 T. Xu, H. Du, H. Liu, W. Liu, X. Zhang, C. Si, P. Liu and K. Zhang, *Adv. Mater.*, 2021, **33**, 2101368.
8 R. Rinaldi, R. Jastrzebski, M. T. Clough, J. Ralph, M. Kennema, P. C. A. Bruijnincx and B. M. Weckhuysen, *Angew. Chem., Int. Ed.*, 2016, **55**, 8164–8215.
9 J. Becker and C. Wittmann, *Biotechnol. Adv.*, 2019, **37**, 107360.
10 S. Chen, Y. Xin and C. Zhao, *ACS Sustainable Chem. Eng.*, 2021, **9**, 15653–15660.
11 R. J. Li, J. Gutierrez, Y.-L. Chung, C. W. Frank, S. L. Billington and E. S. Sattely, *Green Chem.*, 2018, **20**, 1459–1466.
12 Q. He, I. Ziegler-Devin, L. Chrusciel, S. N. Obame, L. Hong, X. Lu and N. Brosse, *ACS Sustainable Chem. Eng.*, 2020, **8**, 5380–5392.
13 S. Afewerki, X. Wang, G. U. Ruiz-Esparza, C.-W. Tai, X. Kong, S. Zhou, K. Welch, P. Huang, R. Bengtsson, C. Xu and M. Strømme, *ACS Nano*, 2020, **14**, 17004–17017.
14 T. Zou, M. H. Sipponen, A. Henn and M. Österberg, *ACS Nano*, 2021, **15**, 4811–4823.
15 L. Zhang, *Formaldehyde: Exposure, Toxicity and Health Effects*, The Royal Society of Chemistry, 2018, ch. 1, pp. 1–19, DOI: 10.1039/9781788010269-00001.
16 T. Salthammer, S. Mentese and R. Marutzky, *Chem. Rev.*, 2010, **110**, 2536–2572.
17 I. Van Nieuwenhove, T. Renders, J. Lauwaert, T. De Roo, J. De Clercq and A. Verberckmoes, *ACS Sustainable Chem. Eng.*, 2020, **8**, 18789–18809.
18 C. Thoma, J. Konnerth, W. Sailer-Kronlachner, T. Rosenau, A. Potthast, P. Solt and H. W. G. van Herwijnen, *ChemSusChem*, 2020, **13**, 5408–5422.
19 C. Scarica, R. Suriano, M. Levi, S. Turri and G. Griffini, *ACS Sustainable Chem. Eng.*, 2018, **6**, 3392–3401.
20 A. H. Hofman, I. A. van Hees, J. Yang and M. Kamperman, *Adv. Mater.*, 2018, **30**, 1704640.
21 L. Liu, Z. Liu, Y. Ren, X. Zou, W. Peng, W. Li, Y. Wu, S. Zheng, X. Wang and F. Yan, *Angew. Chem., Int. Ed.*, 2021, **60**, 8948–8959.
22 C. Cui, C. Shao, L. Meng and J. Yang, *ACS Appl. Mater. Interfaces*, 2019, **11**, 39228–39237.
23 K. G. Latham, L. Matsakas, J. Figueira, U. Rova, P. Christakopoulos and S. Jansson, *J. Anal. Appl. Pyrolysis*, 2021, **155**, 105095.
24 M. Alinejad, C. Henry, S. Nikafshar, A. Gondaliya, S. Bagheri, N. Chen, S. K. Singh, D. B. Hodge and M. Nejad, *Polymers*, 2019, **11**, 1202.
25 P. J. Larkin, in *Infrared and Raman Spectroscopy*, ed. P. J. Larkin, Elsevier, 2nd edn, 2018, pp. 135–151, DOI: 10.1016/B978-0-12-804162-8.00007-0.
26 G. Sivasankarapillai, E. Eslami and M.-P. Laborie, *ACS Sustainable Chem. Eng.*, 2019, **7**, 12817–12824.
27 F. Ferdosian, Z. Yuan, M. Anderson and C. Xu, *Ind. Crops Prod.*, 2016, **91**, 295–301.
28 X. Du, J. Li and M. E. Lindström, *Ind. Crops Prod.*, 2014, **52**, 729–735.
29 R. W. Pow, W. Xuan, D.-L. Long, N. L. Bell and L. Cronin, *Chem. Sci.*, 2020, **11**, 2388–2393.
30 S. Ralph, L. Landucci and J. Ralph, *NMR Database of Lignin and Cell Wall Model Compounds*, 2004.
31 X. Meng, C. Crestini, H. Ben, N. Hao, Y. Pu, A. J. Ragauskas and D. S. Argyropoulos, *Nat. Protoc.*, 2019, **14**, 2627–2647.
32 S. K. Singh, A. W. Savoy, Z. Yuan, H. Luo, S. S. Stahl, E. L. Hegg and D. B. Hodge, *Ind. Eng. Chem. Res.*, 2019, **58**, 15989–15999.
33 R. Katahira, A. Mittal, K. McKinney, X. Chen, M. P. Tucker, D. K. Johnson and G. T. Beckham, *ACS Sustainable Chem. Eng.*, 2016, **4**, 1474–1486.
34 A. Rahimi, A. Ulbrich, J. J. Coon and S. S. Stahl, *Nature*, 2014, **515**, 249–252.
35 L. Wang, L. Lagerquist, Y. Zhang, R. Koppolu, T. Tirri, I. Sulaeva, S. V. Schoultz, L. Vähäsalo, A. Pranovich, T. Rosenau, P. C. Eklund, S. Willför, C. Xu and X. Wang, *ACS Sustainable Chem. Eng.*, 2020, **8**, 13517–13526.
36 T. Phongpreecha, N. C. Hool, R. J. Stoklosa, A. S. Klett, C. E. Foster, A. Bhalla, D. Holmes, M. C. Thies and D. B. Hodge, *Green Chem.*, 2017, **19**, 5131–5143.
37 H. J. Lee, H. K. Lee, E. Lim and Y. S. Song, *Compos. Sci. Technol.*, 2015, **118**, 193–197.
38 C. H. R. M. Wilsens, J. M. G. A. Verhoeven, B. A. J. Noordover, M. R. Hansen, D. Auhl and S. Rastogi, *Macromolecules*, 2014, **47**, 3306–3316.

 This journal is © The Royal Society of Chemistry 2022

Open Access Article. Published on 25 February 2022. Downloaded on 1/23/2026 6:06:52 PM.
This article is licensed under a Creative Commons Attribution-NonCommercial 3.0 Unported Licence.

39 N. A. Nguyen, C. C. Bowland and A. K. Naskar, *Appl. Mater. Today*, 2018, **12**, 138–152.
40 N. A. Nguyen, K. M. Meek, C. C. Bowland, S. H. Barnes and A. K. Naskar, *Macromolecules*, 2018, **51**, 115–127.
41 S. Laurichesse and L. Avérous, *Prog. Polym. Sci.*, 2014, **39**, 1266–1290.
42 I. Ribca, M. E. Jawerth, C. J. Brett, M. Lawoko, M. Schwartzkopf, A. Chumakov, S. V. Roth and M. Johansson, *ACS Sustainable Chem. Eng.*, 2021, **9**, 1692–1702.
43 A. Durmus, A. Kasgoz and C. W. Macosko, *Polymer*, 2007, **48**, 4492–4502.
44 S. Vadukumpully, J. Paul, N. Mahanta and S. Valiyaveettil, *Carbon*, 2011, **49**, 198–205.
45 L. F. M. da Silva, A. Öchsner and R. D. Adams, *Handbook of Adhesion Technology*, Springer Berlin Heidelberg, Berlin, Heidelberg, 2011.
46 E. M. Petrie, An Introduction to Adhesive and Sealants, in *Handbook of Adhesives and Sealants*, McGraw-Hill Professional, New York, NY, USA, 1999, vol. 1, pp. 2–48.
47 S. Ebnesajjad, *Handbook of Adhesives and Surface Preparation*, William Andrew Publishing, Oxford, 2011.
48 Y. Matsushita, S. Wada, K. Fukushima and S. Yasuda, *Ind. Crops Prod.*, 2006, **23**, 115–121.
49 M. Ruths, *Encyclopedia of Tribology*, ed. Q. J. Wang and Y.-W. Chung, Springer US, Boston, MA, 2013, pp. 3435–3443, DOI: 10.1007/978-0-387-92897-5_463.
50 Z. Yuan, G. E. Klinger, S. Nikafshar, Y. Cui, Z. Fang, M. Alherech, S. Goes, C. Anson, S. K. Singh, B. Bals, D. B. Hodge, M. Nejad, S. S. Stahl and E. L. Hegg, *ACS Sustainable Chem. Eng.*, 2021, **9**, 1118–1127.
51 K. Ostendorf, C. Ahrens, A. Beulshausen, J. L. Tene Tayo and M. Euring, *Polymers*, 2021, **13**, 1088.